Smart Structures and Systems, *Vol. 23, No. 2 (2019) 185-194*
DOI: https://doi.org/10.12989/sss.2019.23.2.185

Hybrid parallel smooth particle hydrodynamic for probabilistic tsunami risk assessment and inland inundation

Fritz Sihombing[a] and Marco Torbol*

Ulsan National Institute of Science and Technology (UNIST), Ulsan, Republic of Korea

(Received March 6, 2017, Revised November 22, 2018, Accepted January 16, 2019)

Abstract. The probabilistic tsunami risk assessment of large coastal areas is challenging because the inland propagation of a tsunami wave requires an accurate numerical model that takes into account the interaction between the ground, the infrastructures, and the wave itself. Classic mesh-based methods face many challenges in the propagation of a tsunami wave inland due to their ever-moving boundary conditions. In alternative, mesh-less based methods can be used, but they require too much computational power in the far-field. This study proposes a hybrid approach. A mesh-based method propagates the tsunami wave from the far-field to the near-field, where the influence of the sea floor is negligible, and a mesh-less based method, smooth particle hydrodynamic, propagates the wave onto the coast and inland, and takes into account the wave structure interaction. Nowadays, this can be done because the advent of general purpose GPUs made mesh-less methods computationally affordable. The method is used to simulate the inland propagation of the 2004 Indian Ocean tsunami off the coast of Indonesia.

Keywords: smooth particle hydrodynamic; parallel computing; tsunami risk assessment; probabilistic approach; dynamic analysis

1. Introduction

The 2004 Indian Ocean Tsunami, also named “Boxing Day Tsunami”, occurred on December 26, 2004. An undersea megathrust earthquake with a moment magnitude (Mw) 9.0 caused the tsunami that, within the near field, hit the coasts of Sri Lanka, Indonesia, Thailand, India, and the Maldives. Within the far field, the tsunami hit the coast of Somalia, Tanzania, and other nations on the east Africa coast. It was the second-largest recorded earthquake in history and one of the most catastrophic recorded natural disaster (Borrero *et al.* 2006, Shibayama 2015). The fault ruptured from the western coast of northern Sumatra up until the North Andaman Island for a length of more than 1,400 km. The rupture involved three different segments: the Andaman segment, the Nicobar segment, and the Sumatra segment (Ishii *et al.* 2005). However, only the Sumatra segment, with a length of 420 km, generated the tsunami (Lay *et al*. 2005). Several studies on tsunami wave generation attempted the estimation of the correct fault plane model (Ammon *et al.* 2005, Grilli *et al*. 2007, Lay *et al.* 2005, Wang and Liu 2006). Two models existed: the impulsive fault model and transient fault plane model. In the impulsive fault plane model, the seafloor deforms altogether within a short period of time, and the entire fault line ruptures. In the transient fault plane mode, the seafloor deforms over a longer period of time, and the rupture propagates along the fault (Wang and Liu 2006).

The post-impact tsunami surveys (Borrero 2005, Borrero *et al.* 2006, Borrero *et al.* 2009) measured the inundation heights and the run-up heights and collected information about social loss and economic loss. The surveys are key to understand the mechanism of the tsunami disaster and its wave propagation pattern, when it reached the coastline (Borrero 2005, Shibayama 2015). Borrero *et al.* (2006) conducted the surveys in Banda Aceh in January and February 2005. The team visited several regions in Banda Aceh: Idi, Panteraja, Lhoknga, East of Banda Aceh, Breuh Island, and Deudap Island. Lhoknga, located west of Banda Aceh and on the coastline facing the Indian Ocean, suffered the highest level of damage from the tsunami inundation. The tsunami caused social losses and 230,000 estimated casualties. Field surveys in Banda Aceh recorded a maximum wave run-up of 31.5 m, a sustained flow depth of 12–15 m, in Lhoknga, and an inundated area of 65 km2 between Lhoknga and Banda Aceh (Borrero *et al.* 2006). The World Banks estimated economic losses in the US$ 4.45 billion range (Nazara and Resosudarmo 2007). The Institute for Economics and Social Research (LPEM) at the Faculty of Economics, University of Indonesia, estimated that one-third of the damage inflicted was to public infrastructures (LPEM 2005). The Indonesian National Planning and Development Agency (Bappenas) was developing blueprints for rehabilitation of the basic socioeconomic infrastructures and according to the Asian Development Bank the cost of reconstruction amounted to US$6.5 billion for a 5 years development plan. (Athukorala and Resosudarmo 2005).

The catastrophic impact of a tsunami on both society

*Corresponding author, Associate Professor
E-mail: mtorbol@unist.ac.kr
[a] Ph.D. Student
E-mail: fritzsihombing@unist.ac.kr

http://www.techno-press.com/journals/sss&subpage=7
ISSN: 1738-1584 (Print), 1738-1991 (Online)

and the economic aspects requires a proper and thorough mitigation plan. A tsunami hazard assessment analyzes the relation between the tsunami recurrence rate and its impact. There are two approaches for tsunami hazard assessment: a deterministic approach and probabilistic approach. The deterministic approach, also known as worst case scenario approach, uses the maximum magnitude of an earthquake and/or a tsunami to estimate their impact. The limitation of this approach is the absence of the likelihood of the event. Therefore, the return period of the tsunami event is not taken into consideration (Connor *et al.* 2009). This is a major issue of any worst-case scenario approach and must be addressed by a probabilistic method.

The probabilistic approach of hazard analysis takes into account the return period of the disaster event of interest (Geist and Parsons 2006). The framework of the probabilistic tsunami hazard analysis (PTHA) follows the framework of the probabilistic seismic hazard analysis (PSHA) (Cornell 1968). The PSHA method consists of three steps: delineation of the earthquake sources and its uncertainties, the development of attenuation relationships, and the probabilistic calculations of the earthquake event. The PTHA follows the same concepts, but the earthquake source and the attenuation relationships are substituted by the tsunami generation and its propagation parameters. The hazard parameter is the height of tsunami wave break (Geist and Parsons 2006).

Classic PTHA estimates the realization of tsunami events using mesh-based numerical methods and reproduces the generation of the tsunami wave and its propagation in the open ocean. However, the tsunami wave propagation near the coastline and the inland inundation are challenging due to the coastline complexities: the ocean bathymetry, the inland topography, and the presence of coastal infrastructures. Mesh-based numerical methods are incapable of simulating the inland propagation. Instead, mesh-less numerical methods model the dynamic interaction within the coastline correctly. The smoothed particle hydrodynamic (SPH) method is a particle method, is a mesh-less numerical method, does not require a grid and/or a mesh to calculate the derivatives, and can solve complex physic problems in three dimensions where mesh-based methods failed to perform (Gingold and Monaghan 1977, Lucy 1977). The main drawback of mesh-less methods is their computational cost that hindered their wide applications—up to now.

This study performs PTHA over the Lhoknga region, in Aceh, for tsunami events generated by submarine earthquakes along the Sumatra segment of Sumatra-Andaman subduction zone. The study also estimates the tsunami wave break and the inland inundation of the 2004 Indian Ocean Tsunami in the Lhoknga region using coupled mesh-based, in the far-field, and mesh-less numerical methods, in the near-field. Last, the study compares the estimated tsunami wave break and the data from the field surveys to validate the coupled methods. General purpose GPU (GPGPU) massive parallel computing overcomes the massive computation required by the mesh-less method.

This paper presents in section 2 the method used, the tsunami mechanism, examples of mesh-based numerical method, the SPH method, and the PTHA; in section 3, it presents the results of the simulated tsunami wave, the PTHA, and the tsunami inundation; last in section 4, it presents a discussion and our conclusions.

2. Method

This study performs the probabilistic tsunami hazard assessment of Lhoknga region, Aceh. The area is well known because it was severely affected by the 2004 Indian Ocean tsunami. The tsunami wave spread over 1 km inland and reached heights up to 20 – 25 m. The survey recorded the sustained flow at shoreline at 13 m. The wave also impacted two large ships on Lhoknga coastline: one was dragged inland, and one was capsized (Borrero 2005, Borrero *et al.* 2006). The study models the mechanisms of tsunami event: generation, propagation, and inundation. It considers only the contribution from the Sumatra segment of the subduction area that ruptured, which is the only one that generated a tsunami wave. The simulation is performed through a numerical method. The method takes into account all mechanisms of the tsunami event. Finally, the study derives the tsunami hazard curve of Lhoknga region by adopting PSHA method and estimates the inland inundation.

2.1 Tsunami mechanism

A tsunami wave is caused by a large displacement in a column of water in the ocean due to a disturbance in the seafloor. The possible sources of the disturbance are submarine earthquakes, submarine landslides, volcanic activities, extreme weather, and asteroid impact (Egorov 2007, Lowe and de Lange 2000, Rabinovich *et al.* 2009, Ward 2001, Ward and Asphaug 2000). A submarine earthquake is the most common source (Bernard and Robinson 2009), but not every submarine earthquake generates a tsunami. Vertical movement of the sea floor causes disturbance on the body of water located above. A thrust-type earthquake, which occurs within a subduction zone, uplifts the sea floor. This movement is similar to a paddle and displaces a finite body of water above the ruptured seafloor. Normal fault-type earthquakes can also generate tsunami waves of moderate intensity. Instead, strike-slip earthquakes cannot generate tsunami waves, because the movement of the crust in the horizontal direction does not perturb the body of water above it. An earthquake that generates tsunami waves is called tsunamigenic.

The rupture of the seafloor by a tsunamigenic earthquake displaces a large amount of water. The displacement creates tsunami waves that spread in all directions. In the far field, the length of such a wave can reach hundreds of kilometers, but its height is less than a meter. A tsunami wave is classified as a shallow water wave that propagates for thousands of miles in the open ocean with minimum energy loss (Dao and Tkalich 2007). Tsunami waves radiate perpendicularly to the fault line. The friction between the tsunami wave and the ocean bathymetry (submarine ridges, plateaus, and seamounts) reduces the energy of the wave and affects both the propagation direction and the overall pattern. The speed of a tsunami wave can be estimated by a simple relationship with the water depth: it is square root of the water depth (Power 2013).

The studies on the 2004 Indian Ocean tsunami found that, in the open ocean, the wavelength magnitude of the leading wave was in the order of a 100 km and, in the shallow water near the shore, decreased to 10 km. The height, instead in the open ocean, was between 1 and 2 m, where the water depth was more than 3,000 m, and raised drastically, near the shore. Because the nonlinearity between the wave length and wave height was small, it was ignored (Wijetunge *et al.* 2008).

The final part of a tsunami mechanism is the inundation: the wave breaks on the coastline and propagates inland, flooding everything. The inundation is the crucial part, where the tsunami causes catastrophic impact to infrastructures and casualties. The inundation area can be measured by: 1) field survey, 2) lab experiments, and 3) numerical models (Lee 2011). The estimation of the inundation area using numerical models is complicated because many variables must be considered: the bathymetry, the topography, the elevation of the coastline, and the interaction with the infrastructures. The locality property of the inundation makes the tsunami assessment a challenging process (Arcas and Segur 2012).

2.2 Existing tsunami numerical models

In a tsunami mitigation plan, the most important part is the estimation of the tsunami hazard. The information provided by a tsunami hazard can be used to plan the evacuation area, to develop early warning system, and to determine the focus area for tsunami awareness and educational programs. In areas with frequent occurrence of tsunamis, historical tsunami catalogs can be used to estimate the empirical relationship of tsunami events; but, in most of places, there are not enough historical records to build a reliable catalog. An international collaboration was initiated in 1989 between the JUGG Tsunami Commission and the United Nations Intergovernmental Oceanographic Commission (IOC). The collaboration produced a method to create tsunami inundation maps. This method is accepted worldwide. In the same year, the Tsunami Inundation Modeling Exchange Program (TIME-P) was established. The scope of this program was to transfer the knowledge about tsunami inundation mapping technology for application by the broader audience (Bernard 2001).

The need of creating comprehensive tsunami mitigation plans encouraged progresses in the tsunami modeling by several national agencies. The National Oceanic and Atmospheric Administration (NOAA) in the USA formed The National Tsunami Hazard Mitigation Program (NTHMP) in 1994. The aim of the program was to develop a plan for a tsunami warning system that reduced the risk to coastal residents. In 2005, NTHMP developed a standardized and coordinated tsunami hazard and risk assessments for all coastal regions of the U.S. and its territories.

Even though the occurrence of earthquakes is random, it is possible to estimate the tsunami waves generated by tsunamigenic earthquakes. However, a standard method is required to avoid overestimating such waves. The overestimation of a tsunami wave causes unnecessary evacuation and mass panic, which leads to social disturbance. The reliability of a tsunami model is a serious issue, and standardization is a problem when developing a tsunami numerical model. NOAA employed several models for the tsunami hazard assessment. The models are: TUNAMI-N2 (Imamura F 1996), Cornell multigrid coupled tsunami model (COMCOT) (Wang 2009), and MOST (Method Of Splitting Tsunami) (Titov and Gonzalez 1997). The models used by these methods are a modified leapfrog finite-difference scheme to solve (both linear and nonlinear) shallow-water equations. The models have been through a long process of validation and verification (Synolakis *et al.* 2008).

2.2.1 COMCOT

COMCOT stands for Cornell multigrid coupled tsunami model, developed at Cornell University. The model has been used to study historical tsunami event such as: the 1960 Chilean tsunami (Liu *et al.* 1995b), the 1992 Flores Islands tsunami (Liu *et al.* 1995a), the 2003 Algeria Tsunami (Wang and Liu 2005), and the 2004 Indian Ocean tsunami (Wang and Liu 2006).

The numerical scheme is an explicit leap-frog finite difference method. The source of the tsunami generation can be an earthquake fault (tsunamigenic earthquake), a submarine landslide, a wave maker, or a custom event. For the tsunamigenic earthquake, the framework for the seafloor displacement is based on either Mansinha and Smylie’s theory or Okada’s theory. The parameters for a tsunamigenic earthquake fault are latitude and longitude of the epicenter, focal depth, length and width of the fault plane, dislocation, strike angle, slip angle, and dip angle.

2.2.2 TUNAMI

TUNAMI was initially developed by Disaster Control Research Center in Tohoku University. Motivated by the Tsunami Inundation Modeling Exchange (TIME) program in 1989 and to empower the tsunami mitigation program in the tsunami-prone countries by providing reliable tsunami simulation program, TUNAMI has been used to simulate tsunami events in the Pacific, the Atlantic, and the Indian Oceans. The model has been used to study the 1945 Arabian Sea tsunami (Jaiswal *et al.* 2009), the historical tsunami in Eastern Mediterranean (Yolsal-Cevikbilen and Taymaz 2012), the 1992 Flores Island tsunami (Imamura *et al.* 1995), and the 2011 Tohoku tsunami (Mas *et al.* 2012).

The numerical scheme used in TUNAMI is similar to the scheme used in COMCOT: it is an explicit leap-frog finite difference scheme. To model the generation of tsunami wave one must define the parameters of tsunamigenic earthquake fault. In TUNAMI, a routine converts real fault data and generate the tsunami wave. The generated tsunami wave is used as the initial wave in the TUNAMI model. The parameters required for the fault input are the bathymetry of the area, the coordinates of the starting point and the end point of the fault, the width of the fault in meters, the dip direction, the dip angle, the slip angle, the dislocation, and the depth in meters.

2.2.3 MOST

MOST is an abbreviation for Method of Splitting Tsunami model. Developed by Pacific Marine Environmental Laboratory (PMEL) and University of Southern California; it is the standard model at the NOAA Center for Tsunami Research (NCTR); it assesses the risk; and it mitigates the potential of tsunami hazard. The MOST model has been used to study the probabilistic tsunami hazard at the Seaside, Oregon (Gonzalez *et al.* 2009), the 2004 Indian Ocean tsunami (Geist *et al.* 2007), the 2006 Tonga tsunami (Tang *et al.* 2008), the 2007 Bengkulu tsunami (Borrero *et al.* 2009), and the 2011 Tohoku tsunami (Wei *et al.* 2013).

The generation of tsunami wave is estimated based on the Okada's theory, and its propagation is modeled with a numerical dispersion scheme and the non-linear shallow-water wave equations in spherical coordinates. Another feature of MOST is the Coriolis terms that are included in the numerical model. For the generation of the tsunami wave, the vertical displacement of the ocean floor is the input. The input parameters include the location and the magnitude of the tsunamigenic earthquake.

2.3 Smoothed particle hydrodynamic method

In the beginning, the smoothed particle hydrodynamic (SPH) method was used to simulate non-axisymmetric phenomena in astrophysics (Gingold and Monaghan 1977, Lucy 1977). SPH is a particle method and is mesh-less so does not requires a grid and/or a mesh to calculate the derivatives. It can solve complex physic problems in three dimension, where mesh-based methods failed to perform (Monaghan 1992). The SPH method estimated the flow quantity (*f*) given by

$$f\left(x\right)=\sum_{j} f_j W\left(x-x_j\right)\mathrm{V}_j \tag{1}$$

where V_j is the volume of the *j*th particle located at x_j with scalar quantity f_j, $W(x-x_j)$ is the weighting function, which is known as the smoothing kernel.

The smoothing kernel is specified by an analytical expression, and its evaluation in the Eq. (1) is straightforward. This study uses the Wendland kernel. The other available kernel is the cubic spline, which has a few issues related to the inflexion points in the derivation estimation. The Wendland kernel formula is

$$W\left(x-x_j\right)=C_N\left(1-\frac{q}{2}\right)^4\left(2q+1\right)\ 0\le q\le 2 \tag{2}$$

where $q=r/h$, $r=|x\text{-}xj|$, and, in 3-D, $C_N=21/(16\pi h^3)$. The kernel has a characteristic smoothing length (h) that defines the region of influence. In this study, *h* is set to be $0.866\Delta x$, where Δx is the initial particle spacing. When simulating fluid flow, the SPH method is based on a discrete particle representation of the Navier-Stokes equation in a Langrangian formulation, given by

$$\frac{d\rho}{dt}=-\rho\nabla.\mathrm{u} \tag{3}$$

$$\frac{du}{dt}=-\frac{\nabla P}{\rho}+g+\frac{1}{\rho}\left(\nabla.\mu\nabla\right)\mathrm{u} \tag{4}$$

where ρ is density, μ is laminar viscosity, *u* is velocity, *P* is pressure, *g* is gravity, and *t* is time

This study uses DualSPHysics, a software to solve the numerical tsunami inundation model based on SPH method. DualSPHysics was developed by researchers at the Johns Hopkins University (US), the University of Vigo (Spain), the University of Manchester (UK) and the University of Rome, La Sapienza. DualSPHysics was developed upon a fortran SPH implementation, SPHysics. SPHysics code was validated for different problems of fluid-structure interaction

Although it has been proven a robust model to solve these kind of engineering problems, the computational cost of SPH method is high. This hindered its application, because a supercomputer was the only equipment capable of handling and solving a SPH model in a reasonable amount of time. However, recent developments on general purpose graphics processing units (GPGPUs) provided an inexpensive alternative to large and extensive numerical models. DualSPHysics is written in C++ and CUDA C and is capable of executing a parallel computation on both CPUs and GPUs. DualSPHysics is an open-source code, developed and redistributed under the terms of the GNU General Public License as published by the Free Software Foundation. The main purpose of this software is to encourage other researchers to try SPH method (Crespo *et al.* 2015).

Many studies show the capability of SPH method in handling the fluid-structure-interaction problems. Altomare *et al.* (2015) studied the capability of DualSPHysics to estimate the sea wave force on coastal defenses. The study consists of two phases. In the initial validation phase, there are three types of impacts set in the simulation: standing wave on impermeable fully reflective vertical wall, non-breaking waves on vertical structures, and impulsive provoked breaking waves. The second phase is the application to a real-life problem. The study cases are the Zeebrugge Harbor and the Blankenberge Marina located in Belgium. DualSPHysics was used to estimate the wave forces on the coastal structures. The current limitation of DualSPHysics, the simulation of the re-reflected waves, does not hinder its function as an alternative assessment tool that provide reliable data compared with the physical model.

Barreiro *et al.* (2013) performed numerical simulations of a wave-structure interaction using DualSPHysics. The validation was done by comparing the numerical results with an analytical solution and with the available experimental data. The two parameters that were observed are the force due to the wave breaking and the force due to the wave propagation. Following the validation simulation, DualSPHysics was then applied to a real-life environment simulation. The scenario simulated both the wave propagation and the breaking wave at the same time. The wave propagates, approaches the coastline, and breaks upon reaching it. The force exerted on the urban landscape and furniture due to impacting wave were recorded. Furthermore, DualSPHysics provided results of the moment that shows the intensity of impact and its distribution point. This is a very useful feature to understand the interaction between waves and structures during the wave breaking.

Dao *et al.* (2013) observed the impact on a vertical wall of non-breaking wave run-up and the breaking of the solitary wave run-up. The waves are equivalent to a long wave of a tsunami or a storm. The observation was done by comparing the experimental data with the numerical simulation produced using DualSPHysics and Tunami-N2. The observation put emphasis on the mechanism of wave run-up, i.e. wave propagation, wave breaking, wave impact on the structure, and the post impact wave run-down, and the pressure exerted by the wave impacting the wall. The comparison between the simulation results and the experimental observations of the wave propagation shows the capability of DualSPHysics to simulate the different possible scenarios.

2.4 New approach: tsunami wave simulation coupling two methods

Numerical methods are necessary in tsunami hazard assessment. Some of the tsunami numerical schemes are used as the main source of tsunami modeling for the mitigation programs, but challenges for an accurate inland flow model still exist. The coastline complexities and interaction between coastal infrastructures should be addressed in the tsunami model. Because the extended use of SPH model in the fluid flow problem showed promising results, and because several examples of SPH used in the coastal engineering were successful, in this study we used SPH to model the tsunami wave break, the tsunami inundation on the coastline. GPGPU is used to provide the computational power to solve the numerical model in a reasonable amount of time.

To model the tsunami wave and its impact on the coastline three component must be present: a tsunamigenic earthquake source; the ocean bathymetry and inland topography; and the tsunami generation, propagation, and inundation model. This study employs two numerical simulations: COMCOT and DualSPHysics. While COMCOT take cares of the tsunami generation at the source and its propagation over the open ocean, near the coastline, DualSPHysics relieves COMCOT and continues the wave propagation toward the tsunami wave break on the coastline and inland inundation.

In this study, the 2004 Indian Ocean tsunami was simulated using the fault parameter from Wang and Liu (2006). The study shows good agreement between the estimated model and the observed wave height on the open sea. COMCOT was used to model the wave propagation near coastline in Lhoknga, Aceh. The wave propagation was moved to DualSPHysics to observe the tsunami wave height and inundation process on the coastline of Lhoknga, Aceh. The hazard curve was expressed based on the tsunami wave height on the coastline and the magnitude of tsunamigenic earthquake.

2.5 Probabilistic Tsunami Hazard Analysis (PTHA)

PTHA is a framework to determine the likelihood of tsunami event, a key component for comprehensive tsunami hazard assessment (Geist and Parsons 2006). The method for PTHA is based on PSHA. The source of tsunami in PTHA can be everything that caused significant displacement of the body of water. This study only considers the fault that generated 2004 Indian Ocean tsunami.

The tsunami source in PTHA can be located in near-field or far-field (Geist and Parsons 2006). The attenuation relationship in PTHA depends on the wave propagation, bathymetry, and shoaling factor. In this study, the attenuation relationship of tsunami wave is calculated using COMCOT. The effects of the bathymetry and the shoaling factor are included. The good agreement between the tsunami model and the wave height recorded in Wang and Liu (2006) shows the capability of this model to generate tsunami wave based on the fault displacement.

The probability of at least one tsunami event occurring in a certain time period is assumed to follow a time-independent Poisson process. This assumption was adapted from the PSHA framework. The relationship between a tsunami event occurrence rate can be written as

$$P[\mathrm{Y}_T > \mathrm{y}*] = 1 - \mathrm{e}^{-\lambda_{y*}T} \tag{5}$$

where λ_{y*} is the annual mean number of tsunami events per year with wave height exceeding $y*$. The return period of the tsunami event can be estimated by taking the reciprocal of annual frequency of exceedance. The tsunami annual frequency of exceedance is estimated as the sum of the mean number of tsunamigenic earthquake generated tsunamis satisfying $Y > y*$ at the observed location.

$$\mathrm{y}* = \sum N(M \geq M*) \tag{6}$$

where $N(M \geq M*)$ is the annual number of tsunamigenic eartquakes that occurr within the source zone with magnitude larger than $M*$, which is the magnitude of the tsunamigenic earthquake that generates a tsunami event with a wave height $y*$ at the observed location.

This study uses the fault parameters from Wang and Liu (2006) and estimates the magnitude using the Gutenberg-Richter relationship. For a given tsunami event, the probability that a tsunami wave height Y will exceed a particular value y* can be computed using the total probability theorem

$$\begin{aligned} P[Y > y*] &= P[Y > y*|X]P[X] \\ &= \int P[Y > y*|X]\, f_x(X)\, dx \end{aligned} \tag{7}$$

where X is the vector of random variables that influence Y.

In this study, the quantity in X is the tsunamigenic earthquake magnitude. The probability of exceedance can be written as

$$P[Y > y^*] = \int P[Y > y^* | m] f_M(m) dm \quad (8)$$

For a site with more than one potential tsunamigenic earthquake source, each of which has an average rate of threshold magnitude exceedance ϕ the total average exceedance rate for the observed location is given by

$$\lambda_{y^*} = \sum_{i=1}^{N_S} \varphi_i \int P[Y > y^* | m] f_{Mi}(m) dm \quad (9)$$

3. Results

Using the methods presented in the previous section, a tsunami hazard curve is computed for Lhoknga, Aceh. The maximum height of the tsunami wave is calculated from a set of tsunamigenic earthquakes. The PTHA estimates the return period of the tsunami event in Lhoknga, Aceh. The simulation of the tsunami inundation shows the propagation of the tsunami wave in dryland for 2004 Indian Ocean tsunami event.

3.1 Tsunami wave

The 2004 Indian Ocean tsunami originated from the Sumatra-Andaman fault. The earthquake ruptured 1,300 km of the Sumatra-Andaman fault, but not all sections of the ruptured fault generated the 2004 Indian Ocean tsunami. According to Lay *et al.* (2005) the length of the fault section that generated the tsunami was around 420 km in the Sumatra segment. The simulation of tsunami wave generation and propagation follows the study from Wang and Liu (2006) who defined the length of the contributing fault at 200 km with a moment magnitude M_w = 9.1-9.3 and a return period of 600 years (Suppasri *et al.* 2015). In this study, the length of the fault line contributing to the tsunami generation varies. The corresponding moment magnitude given the length of fault line is calculated using the Gutenberg-Richter relationship. The study limits the fault length to less than 700 km, where the corresponding moment magnitude is M_w = 9.53.

A set of fault lengths is prepared and a set of maximum wave inundation at the coastline is computed. First, COMCOT is used to simulate the generation and the propagation of the tsunami wave in the open ocean. The results are presented in Table 1.

The data shows a positive correlation between tsunamigenic earthquake magnitude and the height of the generated tsunami wave height.

However, this does not necessarily mean that the tsunamigenic earthquake with the largest magnitude has the highest inundation wave. If a complete catalogue of tsunamigenic earthquake source in Indian Ocean is available, one can create a comprehensive PTHA of Indian Ocean and target area. For attenuation relationship of PTHA, the COMCOT model already considers the factors affecting the tsunami wave propagation on its routine. This study computes the source of tsunamigenic earthquake from the fault section that generated 2004 Indian Ocean tsunami.

3.2 Probabilistic Tsunami hazard analysis

The most important part of the PTHA is the tsunami hazard curve (Fig. 1). The hazard curve shows the best estimate of the probability of a tsunami event with certain wave height to occur. This information is useful for tsunami disaster mitigation planning and of interest to the industrial/financial sector. The study computed the tsunami hazard curve of the Sumatra-Andaman fault line: it computed the probability of tsunami wave exceed certain height using Eq. (8) and computed the mean annual of exceedance using Eq. (6).

3.3 Tsunami inundation

The last and key part of this study is the simulation of the inland inundation of the 2004 Indian Ocean tsunami using DualSPHysics. The initial value for the wave propagation and inundation are obtained from the

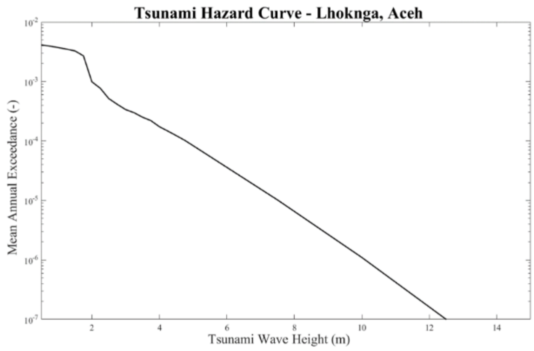

Fig. 1 Tsunami hazard curve of Lhoknga region, Aceh

Table 1 Tsunamigenic earthquake source parameters

Fault Length (km)	Fault Width (km)	Earthquake Magnitude	Tsunami Wave Height (m)
700	150	9.53	7.55
650	150	9.50	7.08
600	150	9.47	7.00
550	150	9.43	6.59
500	150	9.39	5.77
450	150	9.35	4.96
400	150	9.30	3.91
350	150	9.24	2.79
300	150	9.17	2.54
280	150	9.14	2.37
260	150	9.11	2.34
240	150	9.08	2.32
220	150	9.04	2.30
200	150	9.00	2.21
180	150	8.96	2.08
160	150	8.91	1.99
140	150	8.85	1.86
120	150	8.78	1.81
100	150	8.70	1.83

(a)

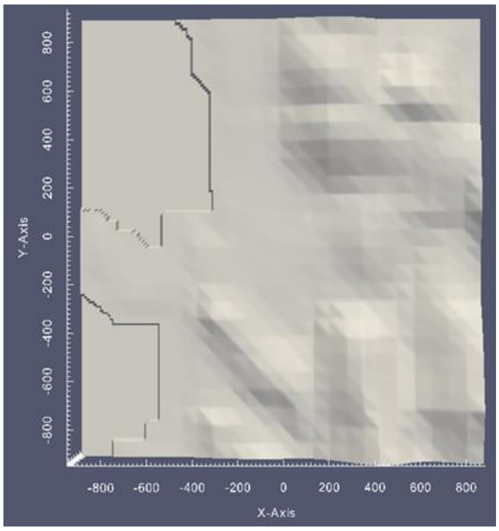

(b)

Fig. 2 (a) Lhoknga coastline and (b) 3D model of Lhoknga coastline

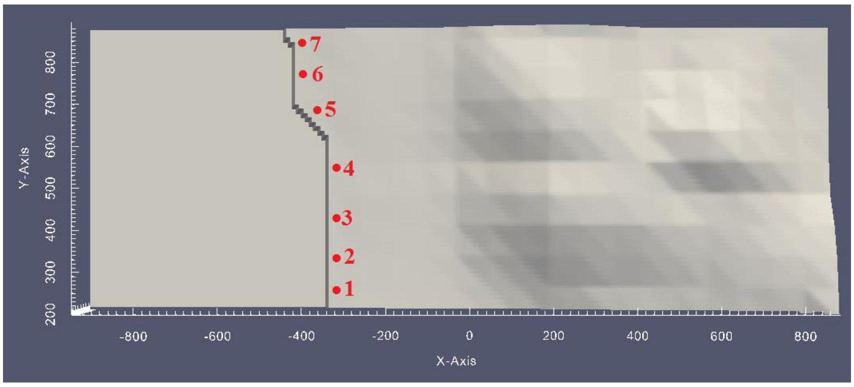

(a)

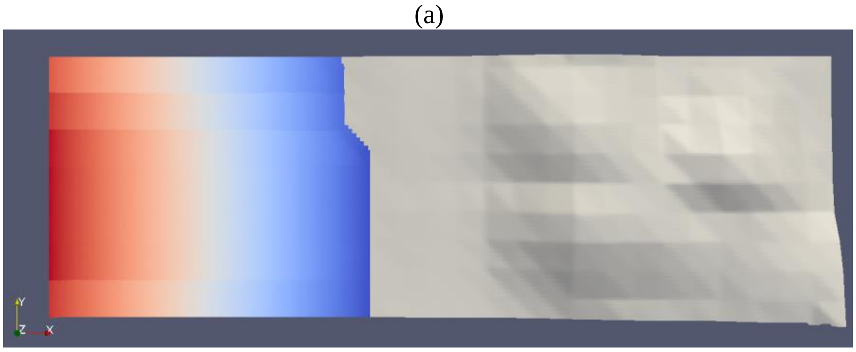

(b)

Fig. 3 (a) Observation points and (b) Initial conditions

COMCOT simulation. Previously, we knew that the coastline complexity was a big challenge to model by the mesh-based numerical method. Therefore, we used DualSPHysics to estimate the tsunami break on Lhoknga coastline and its inland inundation. We then built a 3D model of Lhoknga coastline and used it as the boundary value in the DualSPHysics model. The raw data of Lhoknga coastline is obtained from Google Maps and modified using Sketchup software (Fig. 2(a)). The topography of Lhoknga coastline is modeled using an open-source 3D graphic software, Blender, and it is shown in Fig. 2(b).

Initially, the observation area for tsunami wave break and inland inundation was 1 x 1 km. However, we reduced the observation area into 0.5 x 1 km due to the available global memory on the GPU to allocate the model of the Lhoknga's topography and bathymetry. The final observation model for the tsunami wave break and inland inundation is shown in Fig. 3(a).

We selected 7 different places along the coastline where the waves were observed as shown in Fig. 3(a).

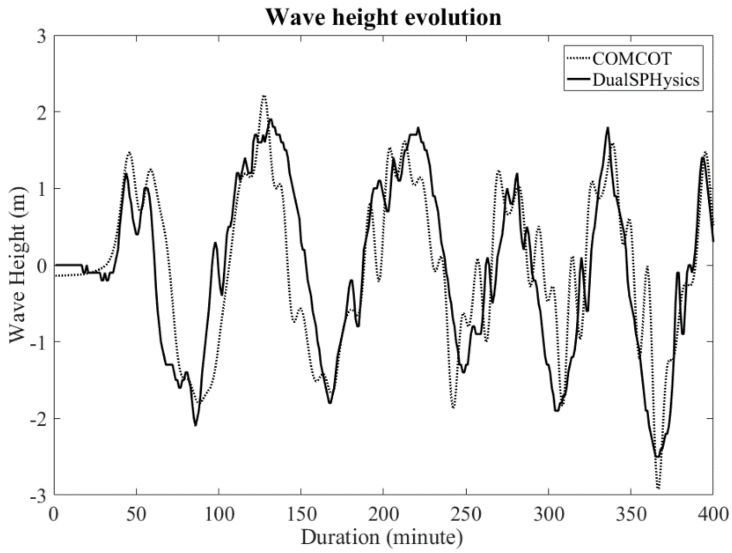

Fig. 4 Comparison of wave height evolution between COMCOT and DualSPHysics at the shift-point

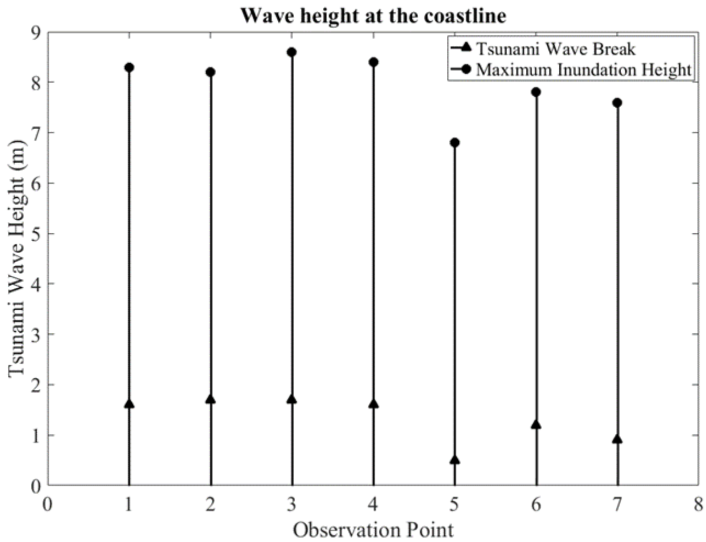

Fig. 5 Records of tsunami wave break and maximum inundation height

This procedure shows the variability of tsunami wave break and inland inundation generated from a tsunami event within a particular location and the capability of DualSPHysics to capture this process. The initial conditions of Lhoknga coastline in DualSPHysics are shown in Figure 3b where the tsunami is not generated yet and the water filled the ocean part in the model.

We simulated the 2004 Indian Ocean tsunami in both DualSPHysics and COMCOT. As mentioned in the method section, the COMCOT simulated the tsunami wave generation and propagation until a certain point near coastline, the shift point. At the shift point, DualSPHysics continues the simulation ant propagates the tsunami wave on the coastline and inland. The wave evolution comparison between COMCOT model and DualSPHysics model at the shift point near coastline is shown in Fig. 4.

The record of tsunami inland inundation height is shown in Fig. 5. This figure shows the variability of tsunami inland inundation, where the similar height of wave break may progress to different height of maximum inundation height. This result can be obtained from the land topography or fluid flow interaction which is captured in the meshless particle method model.

To validate our estimations, we used the field survey of 2004 Indian Ocean tsunami in Lhoknga from Borrero *et al.* (2006). The field survey recorded a maximum tsunami inundation height in the 10m range, while our simulation shows a maximum tsunami inundation height of around 9 m. We think that this discrepancy is due to no real data about the near shore real bathymetry and the accurate topography of Lhoknga. Furthermore, the exact location of the measure of the field survey is unknown.

4. Conclusions

This study performed PTHA and tsunami wave inland inundation of Lhoknga, Aceh region, using COMCOT and

DualSPHysics. Lhoknga is one of the areas severely impacted by the 2004 Indian Ocean tsunami. The method for PTHA in this study is based on PSHA: delineation of the tsunami sources and its uncertainties, the development of attenuation relationships or the propagation relationships, and the probabilistic calculations of the tsunami event.

To model the generation of tsunami from the tsunamigenic earthquake requires knowledge of the involving fault line. The numerical study of tsunami using COMCOT shows that for the 2004 Indian Ocean tsunami, the length of the fault line contributes to the generation of tsunami is 200 km and with a moment magnitude M_w = 9.1-9.3. For PTHA, this study modeled a set of tsunamigenic earthquakes and their return period; used COMCOT + DualSPHysics to propagate the tsunami wave from the far field, to the near field, to the coast, and inland; and built the hazard curve.

This is the first study of its kind that takes a tsunami wave from its point of origin and brings it all the way inland. Previous studies focused either on propagating the wave in the open ocean up to the coast, i.e., mesh-based methods, or on propagating a given violent wave starting from the shoreline and moving inland, i.e., mesh-less based methods. Mesh-based methods are limited by their boundary conditions on the shoreline. Mesh-less methods are limited by the available computational power to shallow-water areas. In this study, we take advantage of mesh-based method for far-field propagation and mesh-less method for near-field and inland propagation. This is a hybrid approach that takes the best of both methods. We used COMCOT to calculate the tsunami wave break and then coupled with DualSPHysics to estimate the inland inundation of tsunami waves. The results of the wave propagation at the end of the COMCOT simulation were the initial conditions of the DualSPHysics simulation. The study showed that although smooth particle hydrodynamics methods are computationally expensive, DualSPHysics can overcome the inland propagation problem.

In this study, we found the wave inundation of the simulations on the coastline shows difference with the available observation data. It should be noted that the simulation included a simple bathymetry topography of Lhoknga. Because the locality aspect of a tsunami plays an important role on the propagation and on the inundation mechanism, a detailed bathymetry and topography is a necessary parameter in tsunami modeling. Furthermore, the exact locations of previous surveys are unknown and caused issues when the simulation data were compared with the observed data.

In this study, the implementation of PTHA by coupling two numerical model shows potential for further development. The complete catalog of earthquake fault, a correct and detailed bathymetry and topography, as well as GPGPU parallel processing are a useful set tool in tsunami hazard risk assessment, particularly PTHA. The PTHA results can be used for tsunami hazard mitigation plan, urban development plan, or in strategic business plan. Finally, the drop-in price for GPGPU parallel computing allows any trained researcher to use SPH models for his region of interest at a reasonable cost, less than a thousand US dollar.

Acknowledgements

This work was supported by Next-Generation Information Computing Development Program through the National Research Foundation of Korea (NRF) funded by the Ministry of Science, ICT (NRF-2016M3C4A7952600).

References

Altomare, C., Crespo, A.J.C., Dominguez, J.M., Gomez-Gesteira, M., Suzuki, T. and Verwaest, T. (2015), “Applicability of Smoothed Particle Hydrodynamics for estimation of sea wave impact on coastal structures”, *Coast. Eng*., **96**, 1-12.

Ammon, C.J., *et al.* (2005), “Rupture process of the 2004 Sumatra-Andaman earthquake”, *Science*, **308**, 1133-1139.

Arcas, D. and Segur, H. (2012), “Seismically generated tsunamis”, *Philos. T. R. Soc. A*, **370**, 1505-1542.

Athukorala, P.C. and Resosudarmo, B.P. (2005), “The Indian Ocean tsunami: Economic impact, disaster management, and lessons”, *Asian Econ. Pap*, **4**, 1-39.

Barreiro, A., Crespo, A.J.C., Dominguez, J.M. and Gomez-Gesteira, M. (2013), “Smoothed particle hydrodynamics for coastal engineering problems”, *Comput. Struct*., **120**, 96-106.

Bernard, E.N. (2001), Recent Developments in Tsunami Hazard Mitigation. Pages 7-15 in (Ed., Hebenstreit, G.T.), *Tsunami Research at the End of a Critical Decade*. Dordrecht: Springer Netherlands.

Bernard E.N. and Robinson, A.R. (2009), Tsunamis. Harvard University Press.

Borrero, J.C. (2005), “Field survey of Northern Sumatra and Banda Aceh, Indonesia after the Tsunami and earthquake of 26 December 2004”, *Seismol. Res. Lett*., **76**, 312-320.

Borrero, J.C., Synolakis, C.E. and Fritz, H. (2006), “Northern sumatra field survey after the December 2004 great Sumatra earthquake and Indian Ocean Tsunami”, *Earthq. Spectra*, **22**, 93-104.

Borrero, J.C., Weiss, R., Okal, E.A., Hidayat, R., Suranto Arcas, D. and Titov, V.V. (2009), “The tsunami of 2007 September 12, Bengkulu province, Sumatra, Indonesia: post-tsunami field survey and numerical modelling”, *Geophys. J. Int*., **178**, 180-194.

Connor, C.B., Chapman, N.A. and Connor, L.J. (2009), Volcanic and Tectonic Hazard Assessment for Nuclear Facilities. Cambridge University Press.

Cornell, C.A. (1968), “Engineering seismic risk analysis”, *B. Seismol. Soc. Am*., **58**, 1583-1606.

Crespo, A.J.C., Dominguez, J.M., Rogers, B.D., Gomez-Gesteira, M., Longshaw, S., Canelas, R., Vacondio, R., Barreiro, A. and Garcia-Feal, O. (2015), “DualSPHysics: Open-source parallel CFD solver based on Smoothed Particle Hydrodynamics (SPH”, *Comput. Phys. Commun*., **187**, 204-216.

Dao, M.H. and Tkalich, P. (2007), “Tsunami propagation modelling - a sensitivity study”, *Nat. Hazard. Earth. Sys*., **7**, 741-754.

Dao, M.H., Xu, H., Chan, E.S. and Tkalich, P. (2013), “Modelling of tsunami-like wave run-up, breaking and impact on a vertical wall by SPH method”, *Nat. Hazard. Earth. Sys*., **13**, 3457-3467.

Egorov, Y. (2007), “Tsunami wave generation by the eruption of underwater volcano”, *Nat. Hazard. Earth. Sys*., **7**, 65-69.

Geist, E.L. and Parsons, T. (2006), “Probabilistic analysis of tsunami hazards”, *Nat. Hazards*, **37**, 277-314.

Geist, E.L., Titov, V.V., Arcas, D., Pollitz, F.F. and Bilek, S.L. (2007), “Implications of the 26 December 2004 Sumatra-Andaman earthquake on tsunami forecast and assessment models for great subduction-zone earthquakes”, *B. Seismol. Soc. Am*., **97**, 249-270.

Gingold, R.A. and Monaghan, J.J. (1977), “Smoothed particle hydrodynamics: theory and application to non-spherical stars”, *Mon. Not. R. Astron. Soc*., **181**, 375-389.

Gonzalez, F.I., *et al.* (2009), “Probabilistic tsunami hazard assessment at Seaside, Oregon, for near- and far-field seismic sources”, *J. Geophys. Res. Ocean.*, **114**, C11

Grilli, S.T., Ioualalen, M., Asavanant, J., Shi, F., Kirby, J.T. and Watts, P. (2007), “Source constraints and model simulation of the December 26, 2004, Indian Ocean Tsunami”, *J. Waterw. Port. Coast*, **133**, 414-428.

Imamura, F. (1996), “Simulation of wave-packet propagation along sloping beach by TUNAMI-code”, *World Scientific*, **3**, 231-241.

Imamura, F., Gica, E., Takahashi, T. and Shuto, N. (1995), “Numerical-simulation of the 1992 Flores Tsunami, interpretation of tsunami phenomena in Northeastern Flores Island and damage at Babi Island”, *Pure. Appl. Geophys*., **144**, 555-568.

Ishii, M., Shearer, P.M., Houston, H. and Vidale, J.E. (2005), “Extent, duration and speed of the 2004 Sumatra-Andaman earthquake imaged by the Hi-Net array”, *Nature*, **435**, 933-936.

Jaiswal, R.K., Singh, A.P. and Rastogi, B.K. (2009), “Simulation of the Arabian Sea Tsunami propagation generated due to 1945 Makran Earthquake and its effect on western parts of Gujarat (India) ”, *Nat. Hazards*, **48**, 245-258.

Lay, T., *et al.* (2005), “The great Sumatra-Andaman earthquake of 26 December 2004”, *Science*, **308**, 1127-1133.

Lee, W.H.K. (2011), Complexity in Earthquakes, Tsunamis, and Volcanoes, and Forecast, Introduction to. Pages 68-78 in (Ed., Meyers, A.R.), *Extreme Environmental Events: Complexity in Forecasting and Early Warning*. New York, NY: Springer New York.

Liu, P.L.F., Cho, Y.S., Briggs, M.J., Kanoglu, U. and Synolakis, C. E. (1995a), “Runup of solitary waves on a Circular Island”, *J. Fluid. Mech*., **302**, 259-285.

Liu, P.L.F., Cho, Y.S., Yoon, S.B. and Seo, S.N. (1995b), Numerical simulations of the 1960 Chilean Tsunami propagation and inundation at Hilo, Hawaii. Pages 99-115 in (Eds. Tsuchiya, Y. and Shuto, N.), *Tsunami: Progress in Prediction, Disaster Prevention and Warning*. Dordrecht: Springer Netherlands.

Lowe, D.J. and de Lange, W.P. (2000), “Volcano-meteorological tsunamis, the c. AD 200 Taupo eruption (New Zealand) and the possibility of a global tsunami”, *Holocene*, **10**, 401-407.

LPEM (2005), Perhitungan Kebutuhan Dana Pembangunan kembali Aceh in (LPEM) IfEaSR, ed. Jakarta.

Lucy, L.B. (1977), A numerical approach to the testing of the fission hypothesis”, *Astron. J.*, **82**, 1013-1024.

Mas, E., Suppasri, A., Imamura, F. and Koshimura, S. (2012), “Agent-based simulation of the 2011 Great East Japan Earthquake/Tsunami Evacuation: An integrated model of tsunami inundation and evacuation”, *J. Nat. Disast. Sci*., **34**, 41-57.

Monaghan, J.J. (1992), “Smoothed particle hydrodynamics”, *Annu. Rev. Astron. Astrophys*., **30**, 543-574.

Nazara, S. and Resosudarmo, B.P. (2007), Aceh-Nias Reconstruction And Rehabilitation: Progress And Challenges At The End Of 2006.

Power, W. (2013), Review of Tsunami Hazard in New Zealand (2013 update). *GNS Science Consultancy Report 2013* 131:222.

Rabinovich, A.B., Vilibic, I. and Tinti, S. (2009), “Meteorological tsunamis: Atmospherically induced destructive ocean waves in the tsunami frequency band”, *Phys. Chem. Earth*, **34**, 891-893.

Shibayama, T. (2015), 2004 Indian Ocean Tsunami. Pages 3-19. *Handbook of Coastal Disaster Mitigation for Engineers and Planners*, Elsevier Inc.

Suppasri, A., Goto, K., Muhari, A., Ranasinghe, P., Riyaz, M., Affan, M., Mas, E., Yasuda, M. and Imamura, F. (2015), “A decade after the 2004 Indian Ocean tsunami: The progress in disaster preparedness and future challenges in Indonesia, Sri Lanka, Thailand and the Maldives”, *Pure. Appl. Geophys.*, **172**, 3313-3341.

Synolakis, C.E., Bernard, E.N., Titov, V.V., Kanoglu, U. and Gonzalez, F.I. (2008), “Validation and verification of tsunami numerical models”, *Pure. Appl. Geophys*., **165**, 2197-2228.

Tang, L., Titov, V.V., Wei, Y., Mofjeld, H.O., Spillane, M., Arcas, D., Bernard, E.N., Chamberlin, C., Gica, E. and Newman, J. (2008), “Tsunami forecast analysis for the May 2006 Tonga tsunami”, *J. Geophys. Res. Ocean*., **113**.C12.

Titov, V.V. and Gonzalez, F. (1997), Implementation And Testing Of The Method Of Splitting Tsunami (MOST) Model. US Department of Commerce, National Oceanic and Atmospheric Administration, Environmental Research Laboratories, Pacific Marine Environmental Laboratory.

Wang, X. (2009), User Manual For COMCOT version 1.7 (first draft), *Cornel University* 65.

Wang, X. and Liu, P.L.F. (2005), “A numerical investigation of Boumerdes-Zemmouri (Algeria) earthquake and tsunami”, *Cmes. Comp. Model. Eng*., **10**, 171-183.

Wang, X. and Liu, P.L.F. (2006), “An analysis of 2004 Sumatra earthquake fault plane mechanisms and Indian Ocean tsunami”, *J. Hydraul. Res*., **44**, 147-154.

Ward, S.N. (2001), “Landslide tsunami”, *J. Geophys. Res-Sol. Ea*, **106**, 11201-11215.

Ward, S.N. and Asphaug, E. (2000), “Asteroid impact tsunami: A probabilistic hazard assessment”, *Icarus*, **145**, 64-78.

Wei, Y., Chamberlin, C., Titov, V.V., Tang, L.J. and Bernard, E. N. (2013), “Modeling of the 2011 Japan Tsunami: Lessons for Near-Field Forecast”, *Pure. Appl. Geophys*., **170**, 1309-1331.

Wijetunge, J.J., Wang, X.M. and Liu, P.L.F. (2008), “Indian Ocean Tsunami on 26 December 2004: Numerical modeling of inundation in three cities on the South Coast of Sri Lanka”, *J. Earthq. Tsunami*, **2**, 133-155.

Yolsal-Cevikbilen, S. and Taymaz, T. (2012), “Earthquake source parameters along the Hellenic subduction zone and numerical simulations of historical tsunamis in the Eastern Mediterranean”, *Tectonophys*., **536**, 61-100.

HJ